

## Seebeck coefficient study on Mn-doped $\text{YBa}_2\text{Cu}_3\text{O}_{7-\delta}$

E. Isaac Samuel and V. Seshu Bai

*School of Physics, University of Hyderabad, Hyderabad 500 046, India*

K. M. Sivakumar and V. Ganesan

*IUC-DAEF, University Campus, Khandwa Road, Indore 452 001, India*

(Received 23 September 1997; revised manuscript received 4 May 1998)

Superconducting samples of  $\text{YBa}_2(\text{Cu}_{1-x}\text{Mn}_x)_3\text{O}_{7-\delta}$  with  $x=0, 0.01, 0.015, 0.02, 0.025, 0.035,$  and  $0.05$  have been prepared and the temperature variation of the Seebeck coefficient,  $S(T)$ , has been measured over a temperature region of 77 to 250 K. The observed features of the results are analyzed in terms of the metallic diffusion model, the Nagaosa-Lee model, and a narrow band model. The physical parameters obtained are discussed. [S0163-1829(99)03310-X]

### I. INTRODUCTION

Over the decade, since the discovery of high- $T_c$  superconductors, study of transport properties has been a rich source for information on Fermi surface, complimented by theory<sup>1-7</sup> and experiments<sup>8-12</sup> alike. Compared to resistivity and Hall coefficient measurements, measurement of Seebeck coefficient is a powerful technique in probing the transport phenomena with minimal distortion arising from the defect structures, etc., which are not the characteristic of the sample studied. Several authors have reported Seebeck coefficients for several systems such as  $\text{La}_{2-x}(\text{Sr},\text{Ba})_x\text{CuO}_4$ ,<sup>13,14</sup>  $\text{YBa}_2\text{Cu}_3\text{O}_{7-\delta}$  (YBCO),<sup>10,12,15-17</sup>  $\text{Bi}_2\text{Sr}_2\text{Ca}_1\text{Cu}_2\text{O}_{8+y}$ ,<sup>18-20</sup>  $\text{Tl}_2\text{Ba}_2\text{Ca}_2\text{Cu}_3\text{O}_y$ ,<sup>21,22</sup> and  $\text{HgBa}_2\text{Ca}_2\text{Cu}_3\text{O}_{8+\delta}$  system,<sup>23,24</sup> and have analyzed the results obtained in the light of energy band calculations to understand the transport mechanism involved.<sup>10,12,25,27</sup>

One of the established consensus on the  $\text{YBa}_2\text{Cu}_3\text{O}_{7-\delta}$  system is that the Cu  $3d$  and O  $2p$  orbitals in the vicinity of the Fermi energy ( $E_f$ ) constitute the superconductivity in this system. This was supported by the angle resolved photoemission experiments<sup>27-29</sup> and the band calculations.<sup>7,30</sup> Consequently doping at the Cu site of  $\text{YBa}_2\text{Cu}_3\text{O}_{7-\delta}$  (Ref. 31) or varying oxygen content<sup>8,9,32</sup> directly alters the charge carriers at the vicinity of  $E_f$  and hence the transport properties. Variation of hole concentration,  $p$ , shows a parabolic effect on  $T_c$ , with  $T_c$  reaching a maximum at an optimum value of hole concentration.<sup>33</sup> Similar effects of hole depletion is observed in  $\text{YBa}_2\text{Cu}_3\text{O}_{7-\delta}$  samples with Pr doped at the Y site.<sup>34</sup> Fisher *et al.*<sup>25</sup> have studied resistivity and thermopower of  $\text{YBa}_2\text{Cu}_{3-x}\text{Co}_x\text{O}_{7-\delta}$  system and proposed the presence of a very narrow band near  $E_f$ . Obertelli *et al.*<sup>9</sup> have brought forth the close correlation existing between the thermoelectric power (TEP) and the superconductivity on several cuprate superconductors. They have also pointed out the crossing over of the sign of the TEP at the vicinity of  $T_c$  maximum where hole doping is optimum. Seebeck coefficient measurements along  $a$  and  $b$  axes of high quality single crystals<sup>15</sup> exhibited a clear distinction between the thermopowers along the  $\text{CuO}_2$  plane and  $\text{CuO}$  chain. The  $a$  axis thermopower has been found to be close to the inplane thermopower of other cuprate superconductors whereas the  $b$

axis Seebeck coefficient, pertaining to the  $\text{CuO}$  chain, is highly sensitive to the oxygen content and is quite temperature independent at high temperatures, indicating that the charge carriers along the chain may be from a very narrow band.

Among the Cu site dopants in YBCO, Mn is expected to display intriguing behavior even at its low solubility limit,<sup>35</sup> as Mn is known to give higher magnetic moment when substituted for Cu in alloys.<sup>36</sup> It was reported that Mn prefers Cu(I) site<sup>37,38</sup> and on doping  $T_c$  remains least altered whereas the magnetic properties deteriorate fast.<sup>39,40</sup> With this background this work is aimed at probing the alteration of the Fermi surface by the Mn dopant and to compare it with the effect of other dopants like Fe that occupy Cu(I) site. In this paper, we present the Seebeck coefficient results on  $\text{YBa}_2(\text{Cu}_{1-x}\text{Mn}_x)_3\text{O}_{7-\delta}$  with  $x$  varying from 0 to 0.05, analyzed in terms of the existing theoretical models. To study the effect of phonon drag on the Seebeck coefficient of this system, metallic diffusion model<sup>24</sup> incorporated with a phonon drag term was used. Nagaosa-Lee model<sup>3</sup> was used to estimate Fermi energy and hole concentration( $p$ ) at the Cu site. Finally, Gasumyants narrow band model<sup>6</sup> was employed to gain a rough insight into the band behavior on doping.

### II. EXPERIMENT

$\text{Y}:\text{Ba}:(\text{Cu},\text{Mn}):\text{O}$  samples of stoichiometric ratio 1:2:(1- $x$ , $x$ )3:7, with  $x$  taking values 0, 0.01, 0.015, 0.02, 0.025, 0.035, and 0.05 were prepared by solid state route. The starting materials of high purity  $\text{Y}_2\text{O}_3$ ,  $\text{Ba}(\text{CO}_3)$ ,  $\text{CuO}$ , and  $\text{MnO}_2$  powders were weighed in the stoichiometric ratio and mixed in an agate mortar thoroughly for about half an hour. The mixture was then fired at 900 °C for ~12 hr. Mixing and presintering at 900 °C was repeated thrice, for homogeneity. The presintered powders were pressed into square pellets of size 1 cm×1 cm×0.5 cm at a uniaxial pressure of ~6 T. These pellets were sintered at 930 °C for 36 h and furnace cooled. These samples were  $\text{O}_2$  annealed at 450 °C for ~60 h. The  $\text{YBa}_2(\text{Cu}_{0.975}\text{Fe}_{0.025})_3\text{O}_{7-\delta}$  sample was also prepared following the aforementioned procedure.

Samples were characterized by x-ray diffraction, resistivity and ac susceptibility measurements. XRD pattern reveals

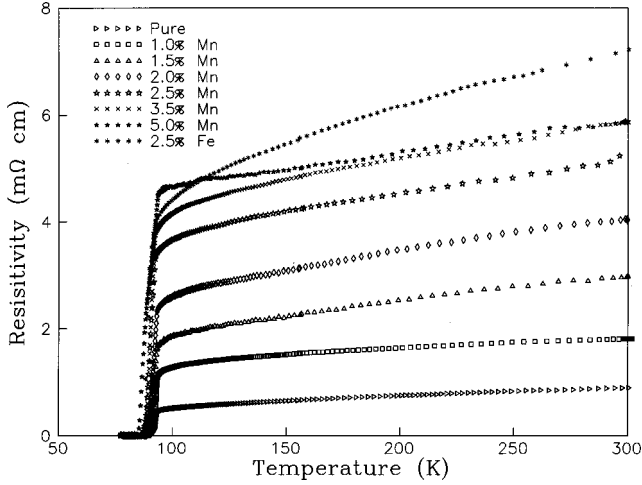


FIG. 1. Temperature variation of resistivity for  $\text{YBa}_2(\text{Cu}_{1-x}\text{Mn}_x)_3\text{O}_{7-\delta}$  samples with  $x=0, 0.01, 0.015, 0.02, 0.025, 0.035,$  and  $0.05$  and  $\text{YBa}_2(\text{Cu}_{0.975}\text{Fe}_{0.025})_3\text{O}_{7-\delta}$  samples.

no secondary phases in the samples studied, except in the case of  $x=0.05$  Mn-doped sample where signature of  $\text{Ba}_3\text{Mn}_2\text{O}_8$  (with intensity less than 5%) is seen at  $\sim 31^\circ 2\theta$  value. The peaks were indexed by comparison with the standard  $\text{YBa}_2\text{Cu}_3\text{O}_{7-\delta}$  pattern and the  $a$ ,  $b$ , and  $c$  parameters were calculated by least square refinement. The values are found to be  $3.82(1)$ ,  $3.88(1)$ , and  $11.67(1)$  Å, respectively, and did not vary beyond the limit of calculation error on Mn doping. For the Fe doped sample the values are  $3.83(1)$ ,  $3.87(1)$ , and  $11.65(1)$  Å, respectively. The calculated values of lattice parameters are in agreement with those reported in literature.<sup>39,40</sup>

The measurement of Seebeck coefficient was carried out following the conventional differential technique. A temperature gradient of 1–3 K was maintained across the sample during the measurement. A Keithley 7002 switching system was employed to control the Keithley 182 nano voltmeter in measuring the voltage across the differential copper-constantan thermocouple and the thermo *emf* ( $\Delta V$ ) developed across the sample. Copper correction was done to obtain the absolute thermopower,  $S$ .

### III. RESULTS AND DISCUSSIONS

Figure 1 shows the temperature variation of resistivity for the  $\text{YBa}_2(\text{Cu}_{1-x}\text{Mn}_x)_3\text{O}_{7-\delta}$  with  $x=0, 0.01, 0.015, 0.02, 0.025, 0.035, 0.05$  and  $\text{YBa}_2(\text{Cu}_{0.975}\text{Fe}_{0.025})_3\text{O}_{7-\delta}$  samples. Resistivity increases monotonically with the dopant concentration, however, the metallicity ( $d\rho/dT$ ) does not show appreciable change. Though the  $\rho(300)$  for the 2.5% Fe-doped sample is higher than that for the 2.5% Mn-doped sample, magnitudes are found to be of the same order. Figure 2 shows the temperature variation of Seebeck coefficient,  $S(T)$ , for the above mentioned samples. The normal state  $S(T)$  shows a change over from a concave behavior for the pure and low dopant concentrations, to a convex behavior when more than 3.5% of Mn and Fe are doped into the sample. The  $S(T)$  for the pure sample is much similar to the  $b$ -axis thermopower reported by Cohn *et al.*<sup>15</sup> on the untwinned  $\text{YBa}_2\text{Cu}_3\text{O}_{7-\delta}$  crystal. Tallon *et al.*<sup>41</sup> have proposed

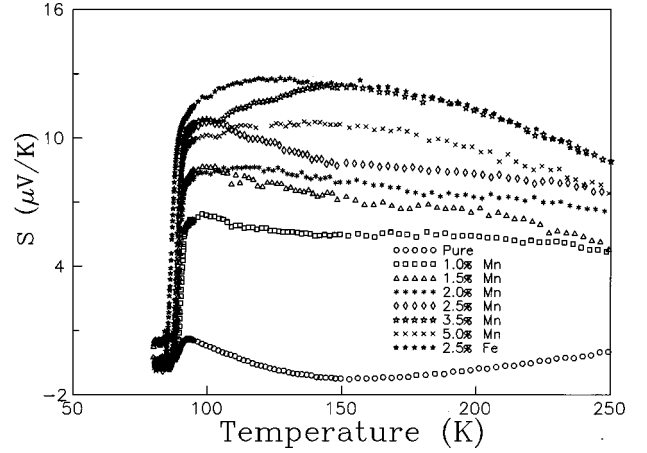


FIG. 2. Temperature variation of the Seebeck coefficient for  $\text{YBa}_2(\text{Cu}_{1-x}\text{Mn}_x)_3\text{O}_{7-\delta}$  samples with  $x=0, 0.01, 0.015, 0.02, 0.025, 0.035,$  and  $0.05$  and  $\text{YBa}_2(\text{Cu}_{0.975}\text{Fe}_{0.025})_3\text{O}_{7-\delta}$  samples.

$S(290)$  to be a reliable gauge for measuring hole concentration, as  $S(290)$  vs hole concentration,  $p$ , follows a universal curve for the high- $T_c$  cuprate superconductors. Following the procedure of Tallon [Eq. (2) in Ref. 41]  $p$  was determined and tabulated (Table I). It can be seen from Table I that  $p$  decreases for increasing dopant concentration. The saturation in  $p$  above 3.5% of Mn could be due to the solubility limit.

### IV. MODELING AND ANALYSIS

Classically the temperature variation of thermoelectric power in metals was explained from the nature of Fermi distribution of the charge carriers under the influence of a temperature gradient. The Seebeck coefficient,  $S$ , calculated from the extra energy required in transporting an electron from the lower temperature end to the higher temperature end is given as<sup>42</sup>

$$S = \int \frac{C_e(T)}{neT} dT, \quad (1)$$

TABLE I. Fit parameters to the metallic diffusion model and  $p$ , the hole concentration, calculated from the  $S(290)$  following Ref. 41.  $a$  is the weightage factor to the metallic diffusion contribution,  $b$  is the weightage factor to the phonon drag contribution, and  $c$  is the additional constant.

Sample	$a$ $\mu\text{V}/\text{K}^2$	$b$ $\mu\text{V}$	$c$ $\mu\text{V}/\text{K}$	$p$
Mn				
0.0	$3.865 \times 10^{-2}$	1010.34	-13.691	0.177
1.0	$1.604 \times 10^{-2}$	460.094		0.145
1.5	$1.643 \times 10^{-2}$	706.167		0.132
2.0	$1.620 \times 10^{-2}$	814.422		0.139
2.5	$1.942 \times 10^{-2}$	896.475		0.123
3.5	$-7.902 \times 10^{-2}$	-1711.178	35.541	0.130
5.0	$-6.012 \times 10^{-2}$	-1083.394	26.860	0.115
Fe				
2.5	$-6.997 \times 10^{-2}$	-1248.157	13.691	0.123

where  $C_e(T)$  is the electronic specific heat,  $n$ , the electron density and  $e$ , the electronic charge. But this simple expression neglects various scattering processes the electron transport encounters in a real situation, arising from crystal defects, phonons, etc.  $S(T)$  under strong scattering conditions<sup>43</sup> is given by

$$S(T) = \frac{k}{e\sigma} \int \sigma(\epsilon) \left( -\frac{\partial f}{\partial \epsilon} \right) \frac{\epsilon - \epsilon_f}{kT} d\epsilon, \quad (2)$$

where  $\sigma(\epsilon)$  is the transport function and the other symbols take the usual notations. Using appropriate transport function  $\sigma(\epsilon)$ , the effect of different transport mechanisms on  $S(T)$  can be derived.

### A. Metallic diffusion model

Several authors have attributed the peak in 100–150 K range to phonon drag effect<sup>10,14,26,44</sup> arising from momentum transfer between the phonons and the charge carriers. Following the Debye's law, the phonon drag is expected to increase as  $T^3$  at low temperature and diminish as  $T^{-1}$  at higher temperatures ( $T > \Theta_D$ , the Debye temperature), because of the anharmonic phonon-phonon scattering, thus accounting for the peak at low temperatures. But the peak observed near  $T_c$  in the high temperature superconductors is at too high a temperature to be accounted for by the above phenomenon as observed in Zn-doped  $\text{YBa}_2\text{Cu}_3\text{O}_{7-\delta}$ .<sup>45</sup> But Cohn *et al.*<sup>26</sup> have argued that at low temperatures, freezing of carrier-optical phonon interaction, responsible for phonon drag at temperatures below 160 K, could result in an enhancement of  $S$  and they have obtained a good fit for the *ab* plane thermopower measured on crystalline YBCO samples. We have fit our experimental results to the thermopower defined as<sup>26</sup>

$$S = aT + \frac{b}{T}. \quad (3)$$

Here, the first term corresponds to the diffusion thermopower and the second term to the phonon drag. For the pure YBCO and the samples with more than 2.5% Mn substitution, an additional constant was used to obtain a good fit. Figure 3 shows the experimental and simulated plots for the thermopower according to metallic diffusion model given by Eq. (3) and the fit parameters are given in Table I. The phonon contribution is enhanced with increasing amount of dopant. The sign of the phonon contribution indicates the direction of momentum transfer<sup>46</sup> and is affected by the hole concentration. In our samples, for  $x > 0.035$  the phonon drag contribution is found to be negative, indicating a reversal in momentum transfer.

### B. Nagaosa-Lee model

Nagaosa and Lee<sup>3</sup> have studied the resonating valence band (RVB) wherein they assume that the fermions and the spinless bosons are coupled by a gauge field. On integrating the fluctuation in the gauge field, the transport properties can be determined from the sum of the boson contribution and the fermion contribution.<sup>47</sup> Thus the Seebeck coefficient can be written as<sup>3</sup>

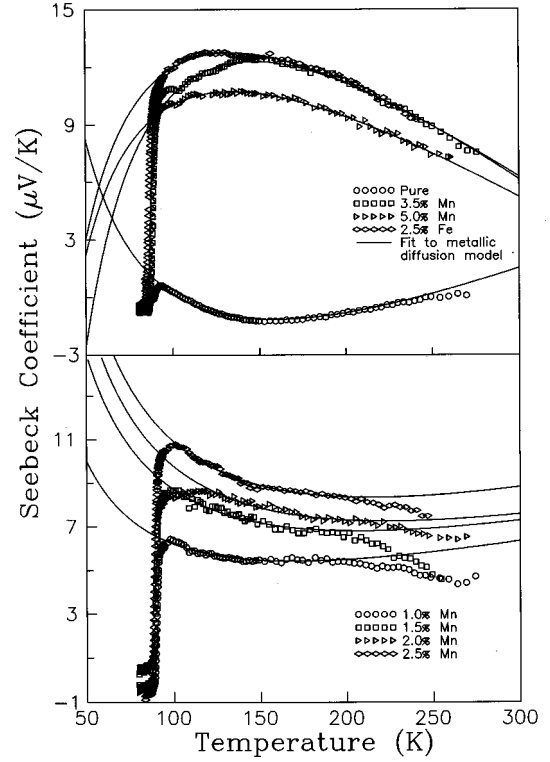


FIG. 3. Metallic diffusion model fit to the  $\text{YBa}_2(\text{Cu}_{1-x}\text{Mn}_x)_3\text{O}_{7-\delta}$  samples with  $x=0, 0.01, 0.015, 0.02, 0.025, 0.035,$  and  $0.05$  and  $\text{YBa}_2(\text{Cu}_{0.975}\text{Fe}_{0.025})_3\text{O}_{7-\delta}$  samples. Solid lines are the theoretical simulations.

$$S = S_f + S_B, \quad (4)$$

where

$$S_f = - \left( \frac{k_B}{e} \right) \frac{k_B T}{E_f}, \quad (5)$$

$$S_B = \frac{k_B}{e} \left( 1 - \ln \frac{2\pi p}{m k_B T} \right). \quad (6)$$

In the above equation for bosonic contribution of thermopower [Eq. (6)] we assume the bosons to be the Cooper pairs and the effective mass is taken as  $2m_e$ . Thus this model gives us a direct correlation between  $S(T)$  and hole concentration,  $p$  and  $E_f$ .

Our experimental results are simulated following the above equation with  $p$  and  $E_f$  as fit parameters. A weightage factor,  $F_{NL}$ , was used to determine the contribution coming from  $S_B$ . Figure 4 shows the simulated plots. The fit parameters are given in Table II and are in the reasonable range, except for the pure sample. For samples up to 2.0% Mn the data could be fitted well in the temperature range of 100–250 K, whereas for samples with dopants above 2.5% Mn, the fit was good only in the temperature range 150–250 K only. As the boson formation due to thermodynamic fluctuations is very unlikely above  $2T_c$ , the bosonic contribution to the Seebeck coefficient,  $S_B$ , will diminish at higher temperatures. Thus for the samples with higher dopant concentration whose measured data could be fitted only at higher temperature range is expected to have low bosonic contribution. This is feebly indicated by the  $F_{NL}$  parameter obtained. But, the

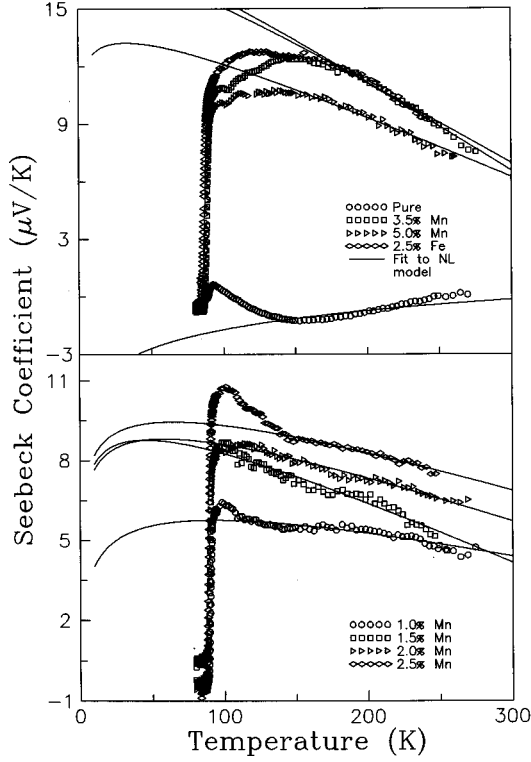


FIG. 4. Nagaosa and Lee model fit to the  $\text{YBa}_2(\text{Cu}_{1-x}\text{Mn}_x)_3\text{O}_{7-\delta}$  samples with  $x=0, 0.01, 0.015, 0.02, 0.025, 0.035,$  and  $0.05$  and  $\text{YBa}_2(\text{Cu}_{0.975}\text{Fe}_{0.025})_3\text{O}_{7-\delta}$  samples. Solid lines represent simulated curves.

abrupt drop by an order in the magnitude of  $p$  estimated from the bosonic contribution of Seebeck coefficient for samples above 2.5% Mn doping and the Fe-doped sample could be due to the fall in  $S_B$ . Also from the low magnitude of the  $F_{NL}$  one can infer the low bosonic contribution. The Fermi energy,  $E_f$ , estimated from the fit decreases from 442 meV for the 1% Mn-doped sample to 146 meV for the 3.5% Mn-doped sample. The  $E_f$  for the 2.5% Fe-doped sample is estimated to be 157 meV. This fall in the  $E_f$  could be an indication of the reduction in the charge carriers on doping, both Mn and Fe alike.

TABLE II. Fit parameters to the Nagaosa and Lee model.  $E_f$  is the Fermi energy,  $p$  is the hole concentration, and  $F_{NL}$  is the weightage factor to the bosonic contribution in the total Seebeck coefficient measured.

Sample	$E_f$ meV	$p$	$F_{NL}$
Mn			
1.0	442.8	0.154	$1.496 \times 10^{-2}$
1.5	271.3	0.167	$1.434 \times 10^{-2}$
2.0	348.6	0.167	$1.439 \times 10^{-2}$
2.5	389.0	0.169	$1.429 \times 10^{-2}$
3.5	146.2	0.033	$1.285 \times 10^{-2}$
5.0	205.2	0.029	$1.382 \times 10^{-2}$
Fe			
2.5	157.9	0.031	$1.302 \times 10^{-2}$

### C. Narrow band model

The temperature independent behavior of thermopower observed in  $\text{YBa}_2\text{Cu}_3\text{O}_{7-\delta}$  system has been explained by considering a narrow band near  $E_f$ .<sup>12,15,25</sup> The saddle point observed in the high resolution angle resolved photo emission experiments on the cuprate superconductors<sup>10,48</sup> point to a logarithmic density of states singularity (Van Hove singularity), close to the  $E_f$ . Gasumyants *et al.*<sup>6</sup> have attempted a quantitative estimation of the transport properties, under the narrow band considerations, using a few phenomenological parameters such as bandwidth ( $W_D$ ), width of the conduction window ( $W_\sigma$ ), and the degree of band filling ( $F$ ). The narrow band could be either a single band in the density of states (DOS), or a narrow peak on a broad background.

On applying the narrow band limitation,<sup>43</sup>  $W \ll k_B T$ , to Eq. (2) the Seebeck coefficient becomes

$$S = \frac{k_B}{e} \ln \left( \frac{F}{1-F} \right) \approx \frac{E - \mu}{eT}. \quad (7)$$

To highlight the influence of the bandwidth, Gasumyants *et al.*<sup>6</sup> have performed the calculations of the transport integrals retaining only the terms up to second or third power in the distribution function expanded as a Taylor's series. Under this approximation,  $S(T)$  for  $W \approx k_B T$  is given as<sup>6</sup>

$$S = -\frac{k_B}{e} \left( \frac{W_\sigma^*}{\sinh[W_\sigma^*]} \left[ e^{-\mu^*} + \cosh[W_\sigma^*] \right] - \frac{\cosh[\mu^*] + \cosh[W_\sigma^*]}{W_\sigma^*} \times \ln \frac{e^{\mu^*} + e^{W_\sigma^*}}{e^{\mu^*} + e^{-W_\sigma^*}} - \mu^* \right), \quad (8)$$

where

$$\mu^* = \frac{\mu}{k_B T} = \ln \frac{\sinh[F W_D^*]}{\sinh[(1-F) W_D^*]},$$

$\mu$  is the chemical potential,

$$W_\sigma^* \equiv W_\sigma / 2k_B T \quad \text{and} \quad W_D^* \equiv W_D / 2k_B T.$$

We have used the above equation to simulate the TEP profiles as a function of temperature and the bandwidth,  $W_D$ . Figure 5(a) shows the temperature variation of  $S$  for varying  $W_D$ . It is evident from the figure that the hump observed at low temperatures in the high- $T_c$  superconductors can be explained in terms the narrowness of the expected band. It can be seen from the plot that as the bandwidth decreases, a broad hump appears on  $S$  vs  $T$  and moves towards the lower temperature as  $W_D$  further decreases. Further, to illustrate the effect of asymmetry added to Eq. (8) we have plotted in Fig. 5(b) the temperature variation of  $S$  for varying  $W_D$  with a small asymmetry factor,  $b=0.02 W_D$ , added to the band near  $E_f$ . In the case of asymmetry added to the band,  $S(T)$  varies just in the same fashion as in the symmetric case but on the negative side, at higher  $W_D$ . And at low  $W_D$ ,  $S(T)$  shows some interesting features such as  $S(T)$  going negative at low temperatures and then raising smoothly to a positive

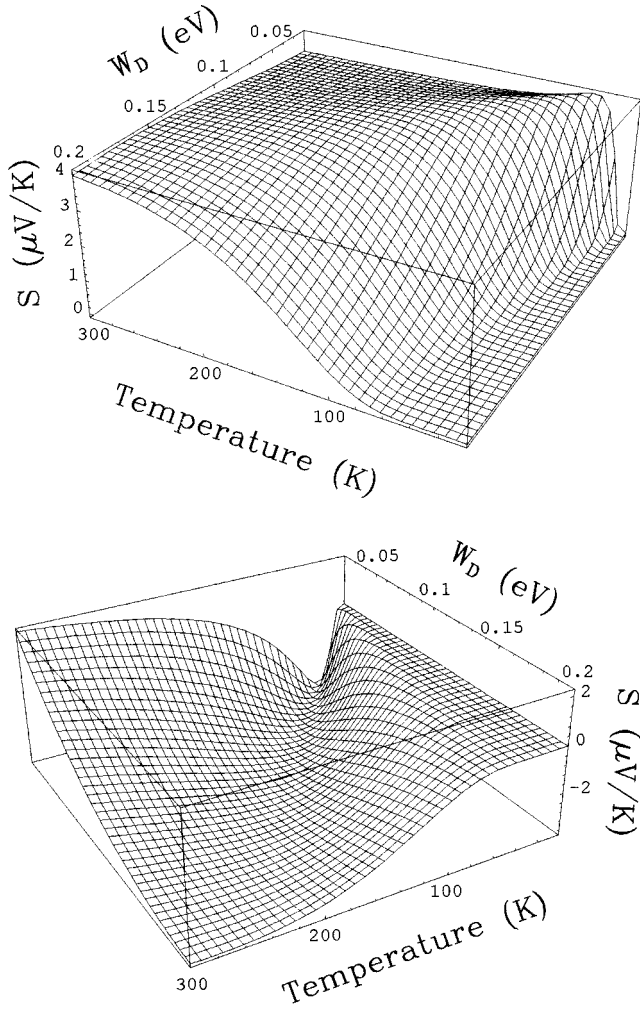


FIG. 5. (a) Temperature variation of Seebeck coefficient for varying bandwidth ( $W_D$ ), given by Gasumyants' narrow band model. (b) Effect of a small asymmetry factor of  $b=0.02W_D$  added about  $E_f$ .

value, until it saturates at high temperatures. This kind of behavior is reported for the  $b$ -axis thermopower measured on untwinned  $\text{YBa}_2\text{Cu}_3\text{O}_{7-\delta}$  single crystals.<sup>15</sup> In our measurements the undoped sample shows a similar behavior.

We have fit the experimental results to Eq. (8) by least square refinement, keeping  $F$ ,  $W_D$ , and  $c$  ( $=W_\sigma/W_D$ ) as fitting parameters. Using a small asymmetry factor, a good fit was obtained for the pure sample. But, the parameters thus obtained are not continuous with those calculated from the symmetric case. Figure 6 shows the calculated and experimental  $S(T)$  plots. The fit parameters are given in the Table III. The width of the narrow band, as seen from the  $W_D$ , increases from 23 meV for the  $x=0.01$  sample to 119 meV for the  $x=0.035$  sample. The band filling factor,  $F$  increases from 0.515 for the 1% Mn-doped sample to 0.524 for the 3.5% Mn-doped sample. Increase in  $F$  or the decrease in hole concentration<sup>6</sup> is in agreement with the variation of  $p$  obtained from the fit to Nagaosa Lee model and the Tallon's universal curve.<sup>41</sup> The conduction window ( $W_\sigma$ ) varies marginally around 35% of  $W_D$ , for the different samples studied but shows no systematic change with doping. This implies Anderson localization<sup>49</sup> is invariant with doping.

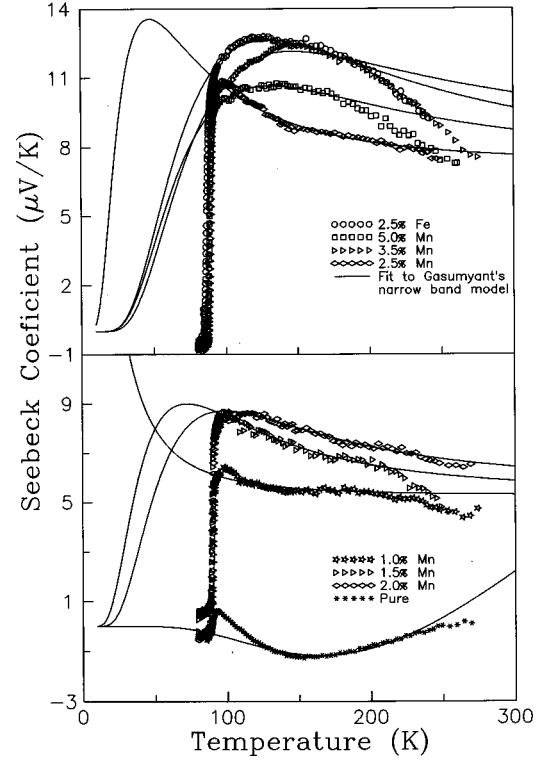


FIG. 6. Gasumyants' narrow band model fit to the  $\text{YBa}_2(\text{Cu}_{1-x}\text{Mn}_x)_3\text{O}_{7-\delta}$  samples with  $x=0, 0.01, 0.015, 0.02, 0.025, 0.035,$  and  $0.05$  and  $\text{YBa}_2(\text{Cu}_{0.975}\text{Fe}_{0.025})_3\text{O}_{7-\delta}$  samples. Theoretical simulations are shown as solid lines.

## V. CONCLUSION

Temperature variation of Seebeck coefficient on  $\text{YBa}_2(\text{Cu}_{1-x}\text{Mn}_x)_3\text{O}_{7-\delta}$  samples with  $x=0, 0.01, 0.015, 0.02, 0.025, 0.035, 0.05$  and a  $\text{YBa}_2(\text{Cu}_{0.975}\text{Fe}_{0.025})_3\text{O}_{7-\delta}$  sample were measured.  $S(290)$  is found to increase monotonically with the dopant concentration, up to 3.5% of Mn which seems to be the solubility limit. Phonon drag component increases with the dopant concentration and momentum transfer changes direction for  $x>0.035$ .  $E_f$  estimated from the Nagaosa and Lee model decreases with increasing dopant concentration. This is due to the decrease in carrier concen-

TABLE III. Fit parameters to the Gasumyants narrow band model.  $f$  is the filling factor,  $W_D$  is the band width, and  $c$  is the ratio of conduction window to the total bandwidth (i.e.,  $W_\sigma/W_D$ ).

Sample	$f$	$W_D$ meV	$c$
Mn			
0.0	0.607	144.778	0.652
1.0	0.515	23.040	0.039
1.5	0.515	72.389	0.323
2.0	0.516	88.578	0.355
2.5	0.521	53.502	0.292
3.5	0.524	119.494	0.385
5.0	0.521	108.963	0.379
Fe			
2.5	0.521	133.089	0.317

tration with doping, which is consistent with the  $p$  calculated from Tallon's universal equation and the degree of band filling  $F$  estimated from Gasumyants' narrow band model. The band parameters calculated from Gasumyants' narrow band model, though they fall in the reasonable range, fail to show any systematic change with doping, but a marginal band broadening and a fall in the hole concentration can be inferred. In all the model calculations, the various parameters obtained for the samples with the Mn dopant above 2.5% are

comparable with those obtained for the Fe-doped sample, showing that the effect of both the dopants, Mn and Fe, at Cu(I) site are similar.

#### ACKNOWLEDGMENTS

One of the authors, E.I.S., gratefully acknowledges University Grants Commission (UGC), India, for the financial assistance.

- <sup>1</sup>P. W. Anderson, *Science* **235**, 1196 (1987).
- <sup>2</sup>S. Massida, J. Yu, and A. J. Freeman, *Physica C* **152**, 251 (1988).
- <sup>3</sup>N. Nagosa and P. A. Lee, *Phys. Rev. Lett.* **64**, 2450 (1990).
- <sup>4</sup>C. M. Varma, P. B. Littlewood, S. Schmitt-Rink, E. Abrahams, and A. E. Ruckenstein, *Phys. Rev. Lett.* **63**, 1996 (1989).
- <sup>5</sup>J. Ruvald and A. Virosztek, *Phys. Rev. B* **42**, 329 (1990).
- <sup>6</sup>V. E. Gasumyants, V. I. Kaidanov, and E. V. Vladimirskaia, *Physica C* **248**, 255 (1995).
- <sup>7</sup>D. M. Newns, C. C. Tsuei, R. P. Huebener, P. J. M. Van Bentum, P. C. Pattnaik, and C. C. Chi, *Phys. Rev. Lett.* **73**, 1695 (1994).
- <sup>8</sup>J. D. Jorgensen, B. W. Veal, A. Paulikas, L. J. Nowicki, G. W. Crabtree, H. Claus, and K. W. Kwok, *Phys. Rev. B* **41**, 1863 (1990).
- <sup>9</sup>S. D. Obertelli, J. R. Cooper, and J. L. Tallon, *Phys. Rev. B* **46**, 14 928 (1992).
- <sup>10</sup>J. W. Cochrane, A. Hartmann, and G. J. Russell, *Physica C* **265**, 135 (1996).
- <sup>11</sup>B. Fisher, J. Genossar, L. Patlagan, G. M. Reisner, and A. Knizhnik, *J. Appl. Phys.* **80**, 898 (1996).
- <sup>12</sup>K. R. Krylov, A. I. Ponomarev, I. M. Tsidilkovski, V. I. Tsidilkovski, G. V. Bazuev, V. L. Kozhevnikov, and S. M. Chesnitski, *Phys. Lett. A* **131**, 203 (1988).
- <sup>13</sup>C. Uher, A. B. Kaiser, E. Gmelin, and I. Waltz, *Phys. Rev. B* **36**, 5676 (1987).
- <sup>14</sup>M. Sera and M. Sato, *Physica C* **185-189**, 1339 (1991).
- <sup>15</sup>J. L. Cohn, E. F. Skelton, and S. A. Wolf, *Phys. Rev. B* **45**, 13 140 (1992).
- <sup>16</sup>P. Gerdanian and C. Picard, *Physica C* **246**, 145 (1995).
- <sup>17</sup>A. B. Kaiser and C. Uher, in *Studies in High Temperature Superconductors*, edited by A. V. Narlikar (Nova Science, New York, 1990), Vol. 7.
- <sup>18</sup>L. Forro, J. Lukatela, and B. Keszer, *Solid State Commun.* **73**, 501 (1990).
- <sup>19</sup>J. B. Mandal, S. Keshri, P. Mandal, A. Poddar, A. N. Das, and B. Gosh, *Phys. Rev. B* **46**, 11 840 (1992).
- <sup>20</sup>R. Wang, H. Sekine, and H. Jin, *Supercond. Sci. Technol.* **9**, 529 (1996).
- <sup>21</sup>Y. Xin, K. W. Wang, C. X. Fan, Z. Z. Sheng, and F. T. Chang, *Phys. Rev. B* **48**, 557 (1993).
- <sup>22</sup>N. Mitra, J. Trefny, B. Yarar, G. Pine, Z. Z. Sheng, and A. M. Hermann, *Phys. Rev. B* **38**, 7064 (1988).
- <sup>23</sup>C. K. Subramaniam, M. Paranthaman, and A. B. Kaiser, *Phys. Rev. B* **51**, 1330 (1995).
- <sup>24</sup>Y. T. Ren, J. Clayhold, F. Chen, Z. J. Huang, X. D. Qiu, Y. Y. Sun, R. L. Meng, Y. Y. Xue, and C. W. Chu, *Physica C* **217**, 6 (1993).
- <sup>25</sup>B. Fisher, J. Genossar, L. Patlagan, and G. M. Reisner, *Phys. Rev. B* **48**, 16 056 (1993).
- <sup>26</sup>J. L. Cohn, S. A. Wolf, V. Selvamanickam, and K. Salama, *Phys. Rev. Lett.* **66**, 1098 (1991).
- <sup>27</sup>T. Takahashi, H. Matsuyama, H. K. Yoshida, Y. Okabe, S. Hosoya, H. Seki, H. Fujimoto, M. Sato, and H. Inokuchi, *Phys. Rev. B* **39**, 6636 (1989).
- <sup>28</sup>R. Manzke, T. Buslaps, R. Claessen, M. Skibowski, and J. Fink, *Physica C* **162-164**, 1381 (1989).
- <sup>29</sup>C. G. Olson, R. Liu, D. W. Lynch, R. S. List, A. J. Arko, B. W. Veal, Y. C. Chang, P. Z. Jiang, and A. P. Paulikas, *Phys. Rev. B* **42**, 381 (1990).
- <sup>30</sup>S. Massida, J. Yu, and A. J. Freeman, *Physica C* **152**, 251 (1988).
- <sup>31</sup>J. M. Tarascon, P. Barboux, P. F. Miceli, L. H. Greene, G. W. Hull, M. Eibschutz, and S. A. Sunshine, *Phys. Rev. B* **37**, 7458 (1988).
- <sup>32</sup>R. J. Cava, A. H. Hewat, E. A. Hewat, B. Batlogg, M. Marezio, K. M. Rabe, J. J. Krajewski, W. F. Peck, Jr., and L. W. Rupp, Jr., *Physica C* **165**, 419 (1990).
- <sup>33</sup>M. R. Presland, J. L. Tallon, R. G. Buckley, R. S. Liu, and N. E. Floer, *Physica C* **176**, 95 (1991).
- <sup>34</sup>A. P. Goncalves, I. C. Santos, E. B. Lopes, R. T. Henriques, M. Almeida, and M. O. Figueiredo, *Phys. Rev. B* **37**, 7476 (1988).
- <sup>35</sup>R. F. Jardim and S. Gama, *Physica C* **159**, 306 (1989).
- <sup>36</sup>J. S. Dugdale, *The Electrical Properties of Metal and Alloys - The Structure and Properties of Solids* (Arnold, London, 1977), Vol. 5, p. 182.
- <sup>37</sup>J. Yang, B. Zhang, H. Zhou, Y. Ding, L. Jin, C. Ye, Y. Yang, Y. Zha, and W. Yuan, *Solid State Commun.* **70**, 919 (1989).
- <sup>38</sup>N. L. Saini, K. B. Garg, H. Rajagopal, and A. Sequera, *Solid State Commun.* **82**, 895 (1992).
- <sup>39</sup>G. Kallias and D. Niarchos, *Supercond. Sci. Technol.* **5**, 56 (1992).
- <sup>40</sup>I. Dhingra, S. C. Kashyap, and B. K. Das, *J. Mater. Res.* **9**, 2771 (1994).
- <sup>41</sup>J. L. Tallon, C. Bernhard, H. Shaked, R. L. Hitterman, and J. D. Jorgensen, *Phys. Rev. B* **51**, 12 911 (1995).
- <sup>42</sup>H. M. Rosenberg, *Low Temperature Solid State Physics* (Clarendon, Oxford, 1965).
- <sup>43</sup>N. F. Mott and E. A. Davis, *Electron Processes in Noncrystalline Materials* (Clarendon, Oxford, 1979).
- <sup>44</sup>A. B. Kaiser and G. Mountjoy, *Phys. Rev. B* **43**, 6266 (1991).
- <sup>45</sup>V. Radhakrishnan, C. K. Subramanian, V. Sankaranarayanan, G. V. Subba Rao, and R. Srinivasan, *Phys. Rev. B* **40**, 6850 (1989).
- <sup>46</sup>H. J. Trodahl, *Phys. Rev. B* **51**, 6175 (1995).
- <sup>47</sup>L. B. Ioffe and A. I. Larkin, *Phys. Rev. B* **39**, 8988 (1989).
- <sup>48</sup>A. A. Abrikosov, J. C. Campuzano, and K. Gofron, *Physica C* **73**, 214 (1993).
- <sup>49</sup>P. W. Anderson, *Phys. Rev.* **109**, 1492 (1958).